

This article was downloaded by: [Renmin University of China]

On: 13 October 2013, At: 10:22

Publisher: Taylor & Francis

Informa Ltd Registered in England and Wales Registered Number: 1072954 Registered office: Mortimer House, 37-41 Mortimer Street, London W1T 3JH, UK



Journal of Coordination Chemistry

Publication details, including instructions for authors and subscription information:

<http://www.tandfonline.com/loi/gcoo20>

Synthesis, crystal structure, DNA binding, and DNA cleavage of a zinc complex containing N,N-bis(2-pyridylmethyl)amine

Jing Qian ^a, Li-Ping Wang ^b, Wen Gu ^c, Xin Liu ^c, Jin-Lei Tian ^c & Shi-Ping Yan ^c

^a College of Chemistry, Tianjin Normal University, Tianjin 300387, P.R. China

^b Department of Chemistry, Baoding College, Baoding 071000, P.R. China

^c College of Chemistry, Nankai University, Tianjin 300394, P.R. China

Published online: 14 Jul 2011.

To cite this article: Jing Qian, Li-Ping Wang, Wen Gu, Xin Liu, Jin-Lei Tian & Shi-Ping Yan (2011) Synthesis, crystal structure, DNA binding, and DNA cleavage of a zinc complex containing N,N-bis(2-pyridylmethyl)amine, Journal of Coordination Chemistry, 64:14, 2480-2488, DOI: [10.1080/00958972.2011.600124](https://doi.org/10.1080/00958972.2011.600124)

To link to this article: <http://dx.doi.org/10.1080/00958972.2011.600124>

PLEASE SCROLL DOWN FOR ARTICLE

Taylor & Francis makes every effort to ensure the accuracy of all the information (the "Content") contained in the publications on our platform. However, Taylor & Francis, our agents, and our licensors make no representations or warranties whatsoever as to the accuracy, completeness, or suitability for any purpose of the Content. Any opinions and views expressed in this publication are the opinions and views of the authors, and are not the views of or endorsed by Taylor & Francis. The accuracy of the Content should not be relied upon and should be independently verified with primary sources of information. Taylor and Francis shall not be liable for any losses, actions, claims, proceedings, demands, costs, expenses, damages, and other liabilities whatsoever or howsoever caused arising directly or indirectly in connection with, in relation to or arising out of the use of the Content.

This article may be used for research, teaching, and private study purposes. Any substantial or systematic reproduction, redistribution, reselling, loan, sub-licensing,

systematic supply, or distribution in any form to anyone is expressly forbidden. Terms & Conditions of access and use can be found at <http://www.tandfonline.com/page/terms-and-conditions>

Synthesis, crystal structure, DNA binding, and DNA cleavage of a zinc complex containing *N,N*-bis(2-pyridylmethyl)amine

JING QIAN*[†], LI-PING WANG[‡], WEN GU[§], XIN LIU[§],
JIN-LEI TIAN[§] and SHI-PING YAN[§]

[†]College of Chemistry, Tianjin Normal University, Tianjin 300387, P.R. China

[‡]Department of Chemistry, Baoding College, Baoding 071000, P.R. China

[§]College of Chemistry, Nankai University, Tianjin 300394, P.R. China

(Received 24 March 2011; in final form 12 May 2011)

A water-soluble zinc complex, $[\text{Zn}(\text{bpea})\text{Cl}_2]$ (**1**) (bpea = *N,N*-bis(2-pyridylmethyl)ethylamine), was prepared to serve as a nuclease mimic. The complex was characterized by X-ray, infrared, and UV spectroscopy. Interactions of the complex with calf thymus-DNA (ct-DNA) have been investigated by UV absorption and fluorescence spectroscopies; the mode of ct-DNA binding for **1** has been proposed. DNA cleavage activities by **1** were performed in the absence of external agents. The influences of different complex concentrations or reaction times on DNA cleavage were studied.

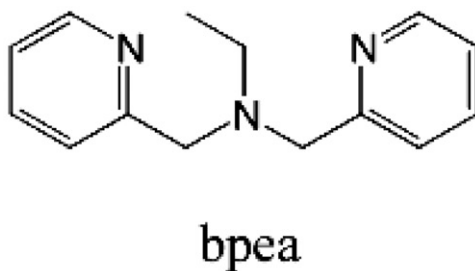
Keywords: Zinc complex; Artificial nuclease; DNA binding; DNA cleavage

1. Introduction

Since the discovery of the first chemical nuclease [1], the design of DNA cleavage agents has been of interest due to their potential use as drugs, tools for molecular biology, and regulators of gene expression [2]. Low molecular weight metal complexes are attractive mimics because of their diverse electronic structures [3]; such studies can help us understand and clarify the role of metal ions in natural nucleases. Large number of studies have been carried out on complexes through an oxidative pathway which requires a co-reactant such as an oxidizing or reducing agent, light, or redox-active metal center [4, 5]. In order to eliminate the possibility of significant cytotoxic side effects of reactive oxygen species, pathways that result in DNA cleavage by hydrolysis mechanisms are preferable [6–8].

Compared with other transition metals, Zn is an ideal agent which can mediate cleavage of phosphate diester backbone, due to its redox inertness and hard Lewis acid properties. Interaction of zinc with nucleobases has been investigated [9] and there have been reports of DNA cleavage [10] and phosphate ester hydrolysis [11] by zinc complexes. However, its nuclease reactivity is somewhat lower than that of the other

*Corresponding author. Email: qianjinger@yahoo.com.cn



Scheme 1. Structure of bpea.

commonly employed metal ions [12], resulting in fewer examples of Zn(II)-based artificial nucleases reported to date [13, 14].

In our attempt to create a Zn(II)-based artificial nuclease, we chose the tridentate nitrogen donor bpea as ligand, as shown in scheme 1, since it is one of the classical ligands in coordination chemistry, and has a potential advantage due to the fact that it can bind to the metal in both facial and meridional fashion [15], and is more flexible than triazacyclononane (TACN) which is strictly facially coordinating [16]. A new zinc complex, **1**, was characterized to serve as a nuclease mimic. Spectroscopic analysis and a detailed investigation into the nuclease activity of **1** are presented.

2. Experimental

2.1. Materials

Ethidium bromide (EB), calf thymus-DNA (ct-DNA), and pBR322 plasmid DNA were obtained from Sigma. Unless stated, all other reagents used in this research were obtained from commercial sources and used without purification. Solvents used in this research were purified by standard procedures. Tris-HCl buffer solution was prepared by using deionized, sonicated, triply-distilled water. Solution of the Zn complex and other reagents used for strand scission was prepared freshly in triply-distilled water before use.

2.2. Measurements

Elemental analyses for C, H, and N were obtained on a Perkin-Elmer analyzer model 240. Infrared (IR) spectroscopy on KBr pellets was performed on a Bruker Vector 22 FT-IR spectrophotometer from 4000 to 400 cm^{-1} . Electronic spectra were measured on a JASCO V-570 spectrophotometer. Fluorescence spectra were recorded on a Cary 300 fluorescence spectrophotometer. The Gel Imaging and Documentation DigiDoc-It System (UVI, England) were assessed using Labworks Imaging and Analysis Software (UVI, England).

2.3. Preparation of ligand and complex

bpea = *N,N*-bis(2-pyridylmethyl)ethylamine was synthesized according to the procedure given in the literature [17, 18].

[Zn(bpea)Cl₂] (1). To an acetonitrile solution (5 mL) of ZnCl₂ · 6H₂O (0.2 g, 1.0 mmol), an acetonitrile solution (15 mL) of bpea (1.0 mmol) was added dropwise with stirring for 3 h at room temperature, and then filtered. Crystals were obtained by slow evaporation of this solution at room temperature (yield: 174 mg, 49%). Anal. Calcd for C₁₄H₁₇Cl₂N₃Zn (363.58) (%): C, 46.25; H, 4.71; N, 11.56. Found (%): C, 46.19; H, 4.54; N, 11.87. FT-IR ν_{\max} (KBr)/cm⁻¹: 3427 (br), 1623 (vs), 1524 (vs), 1417 (vs), 1084 (s). The complex shows good solubility in water and most organic solvents.

2.4. X-ray crystallography

Suitable single crystals were used for X-ray diffraction analysis by mounting on the tip of a glass fiber in air. Data were collected on a Bruker APEX-II CCD diffractometer with Mo-K α ($\lambda = 0.71073 \text{ \AA}$) at 21°C. The structure was solved by direct methods using SHELXS-97 and refined by full-matrix least-squares on F^2 using SHELXL-97 [19]. All non-hydrogen atoms were refined anisotropically and all hydrogens were generated geometrically. Molecular graphics were drawn with the program package Diamond.

2.5. DNA binding experiments

By the electronic absorption spectral method, the relative binding of the complexes to ct-DNA was studied in 5 mmol L⁻¹ Tris-HCl/NaCl buffer at pH 7.2. The solution of ct-DNA gave a ratio of UV absorbance at 260 and 280 nm, A_{260}/A_{280} , of 1.89, indicating that the DNA was sufficiently free of protein [20]. The ct-DNA stock solutions of 5 mmol L⁻¹ were prepared in Tris-HCl/NaCl buffer, pH 7.2 (stored at 4°C and used within 4 days after their preparation). The concentration of ct-DNA was determined from its absorption intensity at 260 nm with a molar extinction coefficient of 6600 (mol L⁻¹)⁻¹ cm⁻¹ [21].

By the fluorescence spectral method, the relative binding of the complexes to ct-DNA was studied with an EB-bound ct-DNA solution in 5 mmol L⁻¹ Tris-HCl/NaCl buffer (pH 7.2). The excitation wavelength was fixed at 510 nm and the emission range was adjusted before measurements. The fluorescence intensities at 602 nm were measured at different complex concentrations [22].

2.6. DNA cleavage experiment

Cleavage of supercoiled (SC) pBR322 DNA by **1** was studied by agarose gel electrophoresis. The reaction was carried out by mixing 4 μ L SC DNA (60 μ mol L⁻¹), 2 μ L complex solution, and 4 μ L 50 mmol L⁻¹ Tris-HCl/NaCl buffer (pH 7.2) (a total volume of 10 μ L). The sample was incubated at 37°C, followed by the addition to 2 μ L loading buffer containing 0.25% bromphenol blue, 50% glycerol, 0.61% Tris, and the solution was finally loaded on 1% agarose gel containing 1.0 μ g mL⁻¹ EB. Electrophoresis was carried out for 4 h at 70 V in TBE buffer (Tris/Borate/EDTA).

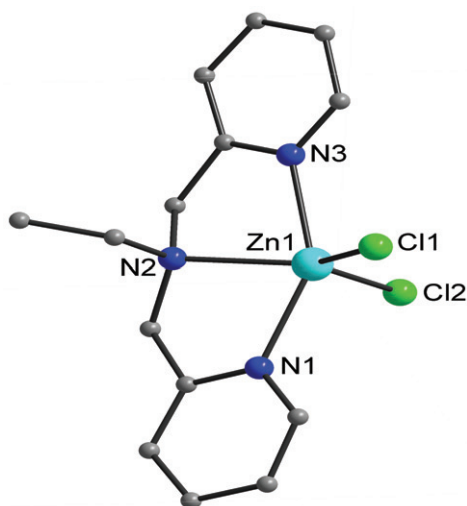


Figure 1. The labeling scheme of $[\text{Zn}(\text{bpea})\text{Cl}_2]$; hydrogens are omitted for clarity.

Bands were visualized by UV light and photographed. The extent of cleavage of the SC DNA was determined by measuring the intensities of the bands using the Gel Documentation System [23]. SC plasmid DNA values were corrected by a factor 1.22, based on the average literature estimate of lowered binding of EB [24].

3. Results and discussion

3.1. Crystal structure

Complex **1** has been structurally characterized by single-crystal X-ray crystallography, IR spectroscopy, and elemental analysis. Complex **1** crystallizes in the monoclinic space group $P2_1/n$ with four molecules per unit cell. Figure 1 shows the labeling Diamond diagram of the neutral molecule. Tables 1 and 2 summarize crystal data and selected bond distances and angles, respectively.

The geometry around zinc is very close to square pyramidal ($\tau = 0.275$) [25, 26], where the tridentate ligand adopts meridional coordination around Zn(II). The equatorial plane has one tridentate ligand (N1, N2, and N3) and Cl1 with Cl2 occupying the axial position. The deviation of zinc is 0.6278 Å from the basal plane. The Zn1–N_{average} distance is 2.189 Å, and the Zn1–Cl1, Zn1–Cl2 distances are 2.257 and 2.272 Å, respectively.

3.2. DNA binding

The potential binding ability of **1** to ct-DNA was studied by UV-Vis spectroscopy; typical titration curves for **1** are shown in figure 2.

The absorption at 272 nm ($\epsilon/\text{dm}^3 \text{mol}^{-1} \text{cm}^{-1}$ 1.39×10^4) for **1** is attributed to an intraligand π – π^* transition. Upon increasing the ct-DNA concentration,

Table 1. Crystallographic data and structure refinement parameters for **1**.

Complex	1
Empirical formula	C ₁₄ H ₁₇ Cl ₂ N ₃ Zn
Formula weight	363.58
Crystal system	Monoclinic
Space group	<i>P</i> 2 ₁ / <i>n</i>
Unit cell dimensions (Å, °)	
<i>a</i>	8.539(4)
<i>b</i>	13.240(6)
<i>c</i>	13.966(6)
α	90
β	91.265(5)
γ	90
Volume (Å ³), <i>Z</i>	1578.6(11), 4
Calculated density (Mg m ⁻³)	1.530
Absorption coefficient (mm ⁻¹)	1.887
<i>F</i> (000)	744
Crystal size (mm ³)	0.20 × 0.20 × 0.20
θ range for data collection	2.12–25.03
Limiting indices	−9 ≤ <i>h</i> ≤ 10; −14 ≤ <i>k</i> ≤ 15; −16 ≤ <i>l</i> ≤ 14
Reflections collected	8278
Independent reflections	2780 [<i>R</i> (int) = 0.0189]
Absorption correction	Semi-empirical from equivalents
Data/restraints/parameters	2780/0/183
Goodness-of-fit on <i>F</i> ²	1.049
Final <i>R</i> indices [<i>I</i> > 2σ(<i>I</i>)]	<i>R</i> ₁ = 0.0233, <i>wR</i> ₂ = 0.0593
<i>R</i> indices (all data)	<i>R</i> ₁ = 0.0287, <i>wR</i> ₂ = 0.0612
Largest difference peak and hole (e Å ⁻³)	0.334 and −0.245

Table 2. Selected bond lengths (Å) and angles (°) for **1**.

Zn(1)–N(1)	2.169(18)	Zn(1)–Cl(1)	2.257(10)
Zn(1)–N(2)	2.232(18)	Zn(1)–Cl(2)	2.272(8)
Zn(1)–N(3)	2.167(18)	–	–
N(3)–Zn(1)–N(1)	149.58(7)	N(3)–Zn(1)–Cl(1)	96.77(6)
N(3)–Zn(1)–N(2)	74.99(6)	N(1)–Zn(1)–Cl(1)	97.67(6)
N(1)–Zn(1)–N(2)	75.58(6)	N(2)–Zn(1)–Cl(1)	133.13(5)
N(3)–Zn(1)–Cl(2)	98.41(5)	N(1)–Zn(1)–Cl(2)	97.56(5)
N(2)–Zn(1)–Cl(2)	107.45(5)	Cl(1)–Zn(1)–Cl(2)	119.42(4)

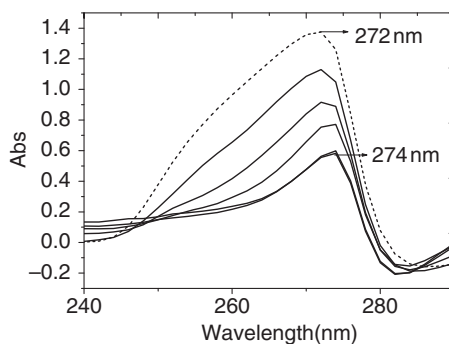


Figure 2. Absorption spectra of **1** (2.21×10^{-4} mol L⁻¹) in the absence (dashed line) and presence (solid line) of increasing amounts of ct-DNA ($0-2.65 \times 10^{-4}$ mol L⁻¹) at room temperature in 5 mmol L⁻¹ Tris-HCl/NaCl buffer (pH = 7.2). The dashed lines indicate the free complex.

hypochromism and red-shift of 2 nm is observed for the maximum, suggesting intercalation between **1** and DNA. Intercalation leads to hypochromism and bathochromism in UV-Vis absorption spectrum involving a strong stacking interaction between an aromatic chromophore and the base pairs of DNA [27]. The extent of the hypochromism is consistent with the strength of intercalation [28]. The value of the intrinsic binding constant $K_b = 2.72 \times 10^4$ for **1** is determined by regression analysis [29]. The value is ~ 100 times lower than those reported for classical intercalators (e.g. EB $\sim 10^6$ (mol L⁻¹)⁻¹) [30], about an order of magnitude lower than affinities of zinc intercalators containing planar ligands [31], but is a little higher than non-intercalating zinc systems such as $[\text{Zn}_2\text{LH}_2(\mu\text{-Cl})\text{Cl}_2(\text{H}_2\text{O})_2]$ [32] (where L is *1H*-pyrazole-3,5-dicarboxy bis(thiosemicarbazide)). The lower K_b observed for the present complex implies that **1** does not intercalate strongly or deeply between the DNA base pairs. So we propose that the lower red-shift observed in the UV-Vis spectra are due to the partial intercalation of the pyridyl ring.

No luminescence is observed for **1** at room temperature in aqueous solution. To further clarify the interaction of **1** with DNA, competitive binding was carried out. EB emits intense fluorescence at 600 nm in the presence of DNA due to its strong intercalation between adjacent DNA base pairs [33]. The enhanced fluorescence could be quenched by the addition of another molecule [34]. Two mechanisms have been proposed to account for this reduction in the emission intensity: the replacement of molecular fluorophores and/or electron transfer [35].

The relative binding of **1** to ct-DNA was studied with an EB-bound ct-DNA solution in 5 mmol L⁻¹ Tris-HCl/50 mmol L⁻¹ NaCl buffer (pH 7.2). Fluorescence intensities at 602 nm (510 nm excitation) were measured at different complex concentrations. The relative binding propensity of the zinc complex to ct-DNA was determined from comparison of the slopes of the lines in the fluorescence intensity *versus* complex concentration plots. As shown in figure 3, the plot of I_0/I *versus* concentration of complex, where I_0 and I represent the fluorescence intensities in the absence and presence of the complex, respectively, the apparent binding constant (K_{app}) was calculated from the equation $K_{\text{EB}}[\text{EB}] = K_{\text{app}}[\text{complex}]$, where the complex concentration was the value at a 50% reduction of the fluorescence intensity of EB and $K_{\text{EB}} = 1.0 \times 10^7$ (mol L⁻¹)⁻¹ ($[\text{EB}] = 4.0 \mu\text{mol L}^{-1}$). The binding constant of the classical intercalator and metallointercalator was 10^7 (mol L⁻¹)⁻¹ [36]. The apparent binding

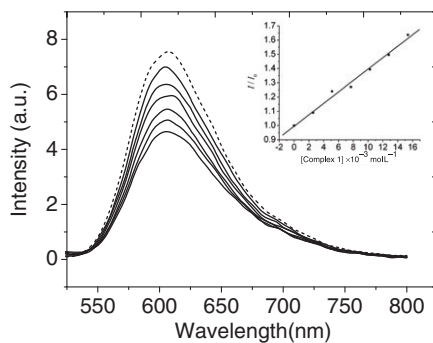


Figure 3. Emission spectra of EB-ct-DNA in the absence and presence of **1** at room temperature. The dashed line indicates EB-DNA.

constant (K_{app}) value for the zinc species is $1.6 \times 10^3 \text{ (mol L}^{-1}\text{)}^{-1}$, indicating that the interaction with DNA is a moderate intercalative mode. The obtained result suggests that EB molecules are replaced by **1**, consistent with the above spectral results suggesting partial intercalation of the pyridyl ring of the ligand, which facilitates DNA binding.

3.3. DNA cleavage

The ability of **1** to cleave DNA was assayed with gel electrophoresis on SC pBR322 plasmid DNA as a substrate in 50 mmol L^{-1} Tris-HCl/ 18 mmol L^{-1} NaCl buffer (pH 7.2) in the absence of external agent. When circular plasmid DNA is subjected to electrophoresis, the fastest migration will be observed for the SC form (Form I). If one strand is cleaved, the SC DNA relaxes to produce a slower-moving nicked circular form (Form II). If both strands are cleaved, a linear form (Form III) is generated which migrates between Forms I and II.

3.3.1. Effect of complex concentration on plasmid DNA cleavage. Concentration-dependent DNA cleavage by **1** was performed. The activity of **1** was assessed by the conversion of DNA from Form I to Form II. Figure 4 shows the results of gel electrophoretic separations of plasmid pBR322 DNA induced by increasing the concentration of **1** in the absence of external agent at pH 7.2 (50 mmol L^{-1} Tris-HCl/NaCl buffer) and 37°C . Upon increasing complex concentrations, the amount of Form I decreases gradually and Form II increases. Under aerobic conditions, when the concentration of **1** reached 3.2 mmol L^{-1} , the SC DNA degraded about 50% (lane 7). It is clear that the degradation of pBR 322 DNA is highly dependent on the concentration of zinc complex used.

3.3.2. Effects of reaction time on plasmid DNA cleavage. The time-dependent cleavage of DNA by **1** was also studied under similar conditions. With the increase in reaction time, amounts of Form II and Form III increased and Form I gradually disappeared. The results show that **1** can effectively cleave the pBR322 plasmid DNA without the addition of external agents, and the cleavage of DNA by **1** is dependent on reaction time, as shown in figure 5. From these experimental results, we find that plots for the appearance of Form II as well as the disappearance of Form I follow pseudo-first-order kinetic profiles and fit well to a single-exponential decay curve, consistent with the general model for enzyme-catalyzed reactions [37]. Fitting the experimental data with first-order consecutive kinetic equations, the rate constants $k_{obs} = 4.72 \pm 0.6 \times 10^{-5} \text{ s}^{-1}$

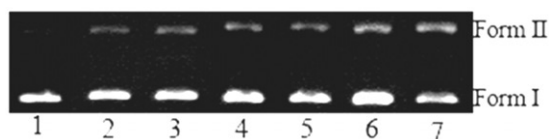


Figure 4. Cleavage of plasmid pBR322 DNA ($40 \mu\text{mol L}^{-1}$, in base pairs) with varying concentrations of **1** at 37°C in Tris-HCl/NaCl buffer (pH 7.2). Lane 1: DNA control; lanes 2–7: DNA + **1** (0.1, 0.2, 0.4, 0.8, 1.6, 3.2 mmol L^{-1} incubation for 6 h), respectively.

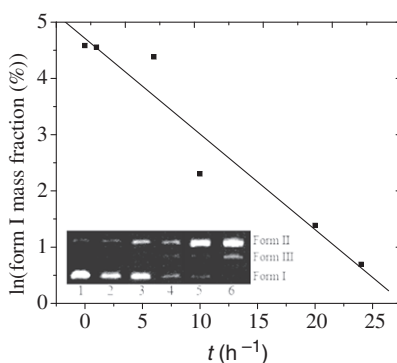


Figure 5. Cleavage of plasmid pBR322 DNA ($60 \mu\text{mol L}^{-1}$, in base pairs) in the presence of 1.6 mmol L^{-1} **1** at various incubation times at pH 7.2 and 37°C . Lane 1: DNA control; lanes 2–6: DNA + **1** (1 h, 6 h, 10 h, 20 h, 24 h).

for the conversion of SC to nicked DNA are obtained for **1**. The cleavage efficiency depends both on the complex concentration and on the reaction time.

4. Conclusions

A water-soluble zinc complex was designed and characterized to serve as a nuclease mimic. The complex displays efficient partial intercalation binding to ct-DNA and chemical nuclease activity in the absence of reducing agent at physiological conditions. Based on the kinetics experiments, complex **1** shows high catalytic activity. Unfortunately, such high reactivity is counterbalanced by moderate affinity for the substrate ($10^3 (\text{mol L}^{-1})^{-1}$) so that long time (h) and higher concentration (mmol L^{-1}) is required to obtain a fast degradation of DNA. Synthesis of higher affinity and reactivity zinc complexes and their kinetic and theoretical studies are in progress.

Supplementary material section

Crystallographic data for the structure analysis in this article have been deposited with the Cambridge Crystallographic Data Centre as supplementary publication, No. of CCDC, 603567.

Acknowledgments

Financial support from the National Natural Science Foundation of China (Grant No. 21001066), the PhD Science Foundation of Tianjin Normal University (Grant No. 52LX28), and the Education Science Foundation of Tianjin City (Grant No. 20070606) are gratefully acknowledged.

References

- [1] D.S. Sigman, D.R. Graham, V. Daurora, A.M. Stern. *J. Biol. Chem.*, **254**, 12269 (1979).
- [2] C.J. Burrows, J.G. Muller. *Chem. Rev.*, **98**, 1109 (1998).
- [3] M. Oivanen, S. Kuusela, H. Lonnberg. *Chem. Rev.*, **98**, 961 (1998).
- [4] D.S. Sigman, A. Mazumder, D.M. Perrin. *Chem. Rev.*, **93**, 2295 (1993).
- [5] C.J. Burrows, S.E. Rokita. *Acc. Chem. Res.*, **27**, 295 (1994).
- [6] M.P. Fitzsimmons, J.K. Barton. *J. Am. Chem. Soc.*, **119**, 3379 (1997).
- [7] A. Sreedhara, J.D. Freed, J.A. Cowan. *J. Am. Chem. Soc.*, **122**, 8814 (2000).
- [8] P. Ordoukhanian, G.F. Hoyce. *J. Am. Chem. Soc.*, **124**, 12499 (2002).
- [9] D. Badura, H. Vahrenkamp. *Inorg. Chem.*, **41**, 6013 (2002).
- [10] A. Nomura, Y. Sugiura. *J. Am. Chem. Soc.*, **126**, 15374 (2004).
- [11] Y. Gupta, G.N. Mathur, M. Parvez, S. Verma. *Bioorg. Med. Chem. Lett.*, **16**, 5364 (2006).
- [12] E.L. Hegg, J.N. Burstyn. *Coord. Chem. Rev.*, **173**, 133 (1998).
- [13] K. Ichikawa, M. Tarani, M.K. Uddin, K. Nakata, S. Sato. *J. Inorg. Biochem.*, **91**, 437 (2002).
- [14] E. Boseggia, M. Gatos, L. Lucatello, F. Mancin, S. Moro, M. Palumbo, C. Sissi, P. Tecilla, U. Tonellato, G. Zagotto. *J. Am. Chem. Soc.*, **126**, 4543 (2004).
- [15] S. Pal, M.M. Olmstead, W.H. Armstrong. *Inorg. Chem.*, **33**, 636 (1994).
- [16] J. Qian, W. Gu, H. Liu, F.X. Gao, L. Feng, S.P. Yan, D.Z. Liao, P. Cheng. *Dalton Trans.*, 1060 (2007).
- [17] S. Pal, M.K. Chan, W.H. Armstrong. *J. Am. Chem. Soc.*, **114**, 6398 (1992).
- [18] K.B. Jensen, C.J. Mckenzie, O. Simonsen, H. Toftlund, A. Hazell. *Inorg. Chim. Acta*, **257**, 163 (1997).
- [19] *SHELXTL 6.10*. Bruker Analytical Instrumentation, Madison, WI, USA (2000).
- [20] J. Marmur. *J. Mol. Biol.*, **3**, 208 (1961).
- [21] M.E. Reichmann, S.A. Rice, C.A. Thomas, P. Doty. *J. Am. Chem. Soc.*, **76**, 3047 (1954).
- [22] J.R. Lakowicz, G. Weber. *Biochemistry*, **12**, 4161 (1973).
- [23] J. Bermadou, G. Pratiel, F. Bennis, M. Girardet, B. Meunier. *Biochemistry*, **28**, 7268 (1989).
- [24] R.P. Hertzberg, P.B. Dervan. *J. Am. Chem. Soc.*, **104**, 313 (1982).
- [25] A.W. Addison, T.N. Rao, J. Reedijk, J. van Rijn, G.C. Verschoor. *J. Chem. Soc., Dalton Trans.*, 1349 (1984).
- [26] S.Q. Bai, E.Q. Gao, Z. He, C.J. Fang, C.H. Yan. *New J. Chem.*, **29**, 935 (2005).
- [27] M. Baldini, M. Belicchi-Ferrari, F. Bisceglie, P.P. Dall'Aglio, G. Pelosi, S. Pinelli, P. Tarasconi. *Inorg. Chem.*, **43**, 7170 (2004).
- [28] S.A. Tysoe, R.J. Morgan, A.D. Baker, T.C. Streckas. *J. Phys. Chem.*, **97**, 1707 (1993).
- [29] A. Wolfe, G.H. Shimer, T. Meehan. *Biochemistry*, **26**, 6392 (1987).
- [30] J.B. Le Pecq, C. Paoletti. *J. Mol. Biol.*, **27**, 87 (1967).
- [31] N. Raman, A. Sakthivel, R. Jeyamurugan. *J. Coord. Chem.*, **63**, 1080 (2010).
- [32] N.V. Kulkarni, V.K. Revankar. *J. Coord. Chem.*, **64**, 725 (2011).
- [33] F.J. Meyer-Almes, D. Porschke. *Biochemistry*, **32**, 4246 (1993).
- [34] B.C. Baguley, M. LeBret. *Biochemistry*, **23**, 937 (1984).
- [35] R.F. Pasternack, M. Cacca, B. Keogh, T.A. Stephenson, A.P. Williams, F.J. Gibbs. *J. Am. Chem. Soc.*, **113**, 6835 (1991).
- [36] M. Cory, D.D. Mckee, J. Kagan, D.W. Henry, J.A. Miller. *J. Am. Chem. Soc.*, **107**, 2528 (1985).
- [37] J.J. Li, R. Geyer, W. Tan. *Nucleic Acids Res.*, **28**, e52 (2000).